Journal of Luminescence 133 (2013) 257–261

Contents lists available at SciVerse ScienceDirect

Journal of Luminescence

journal homepage: www.elsevier.com/locate/jlumin

Mid-IR lasing of iron–cobalt co-doped ZnS(Se) crystals via Co–Fe energy transfer

NoSoung Myoung, Dmitri V. Martyshkin, Vladimir V. Fedorov *, Sergey B. Mirov

Center for Optical Sensors and Spectroscopies and the Department of Physics, University of Alabama at Birmingham, CH 310, 1300 University Boulevard, Birmingham, AL 35294, USA

ARTICLE INFO

Available online 12 October 2011

Keywords:
Mid-IR lasers
Co–Fe energy transfer
Fe:ZnS and Fe:ZnSe crystals
Transitional metal doped lasers

ABSTRACT

We report a spectroscopic characterization of iron–cobalt co-doped ZnS and ZnSe laser crystals over 14–300 K temperature range. Mid-IR Fe^{2+} lasing via Co–Fe energy transfer was demonstrated under cobalt excitation at $^4A_2$–$^4T_1$ transition by 1.56 μm radiation.

1. Introduction

Development of technology of high optical quality gain media based on transition metal (TM) doped ZnSe and ZnS crystals was inspired by a growing demand for room temperature middle infrared (mid-IR) lasers operating over 2–6 μm spectral range for a wide range of applications such as free space optical communication, remote sensing, medical diagnostics, etc. Recently room temperature gain-switched lasing with output energy 20 mJ@ 2.5 μm and 4.7 mJ @ 4.3 μm were reported for chromium and iron doped ZnSe lasers, respectively [1]. Iron doped II–VI lasers operating over 3.7–6 μm range with a high optical efficiency are well documented [2–7]. However, one of the problems limiting practical applications of these lasers is a lack of availability of convenient pump sources. The absorption bands of Fe^{2+} ions in II–VI semiconductors have a maximum between 3 and 4 μm. Currently, the most commonly used pump sources of Fe-II–VI lasers are Er lasers operating near 3 μm. The radiation of 3 μm Er lasers nicely overlaps with iron absorption bands in ZnS and ZnSe crystals but is not suitable for efficient pumping of a Fe:ZnCdTe and Fe:CdMnTe lasers. One of the possible solutions for development of suitable mid-IR iron lasers could be utilization of energy transfer from conveniently pumped donor to laser active iron ions. Energy transfer between transition metal ions and Fe^{2+} in II–VI semiconductors was observed for Cr–Fe [2], Co–Fe [8], and Ni–Fe pairs [9]. In spite of this interest in the energy transfer processes in TM:II–VI crystals, the laser oscillation of Fe^{2+} ions via energy transfer excitation has not been reported yet.

In this paper we report spectroscopic characterization and mid-IR laser oscillation via energy transfer in the Co:Fe:ZnS and Co:Fe:ZnSe co-doped crystals (Co:Fe:ZnS/Se). The energy structure of Co^{2+} and Fe^{2+} ions in tetrahedral crystal field is shown in Fig. 1. Divalent cobalt ions have two strong absorption bands located at 730 and 1600 nm, which could be potentially used for pumping by commercially available bulk, fiber or diode lasers. In this research we focused on spectroscopic characterization of Co:Fe:ZnS and Co:Fe:ZnSe crystals under cobalt excitation at $^4A_2(F)\rightarrow{}^4T_1(F)$ transition. Potentially, excitation of $^4T_1(F)$ state of cobalt ion can result in excitation of two iron ions due to two possible channels of Co → Fe energy transfer. Initially, iron excitation to $^5T_2(D)$ iron state can result from $^4T_1(F)\rightarrow{}^4T_2(F)$ cross-relaxation process. Later, this process can be followed by energy transfer from $^4T_2(F)$ cobalt state. Based on Forster–Dexter theory [10], one can expect a fast energy transfer rate due to a good spectral overlap of Co emission ($^4T_2(F)\rightarrow{}^4A_2(F)$) and Fe absorption ($^5E_2(D)\rightarrow{}^5T_2(D)$) bands . Realization of this excitation mechanism can potentially result in better than 100% quantum efficiency of iron excitation under 1.5 μm pumping.

2. Sample preparation and experimental setup

Co-doped Co:Fe:ZnSe and Co:Fe:ZnS polycrystals with dimension of $10\times10\times1.2\ mm^3$ were fabricated using two-stage thermo-diffusion method. Initial thermal diffusion of cobalt ions was performed in a sealed quartz ampoule at 10^{-5} Torr at annealing temperature of 1000 °C for 16 days. Thermal diffusion of iron ions was performed at the same temperature for 20 days. The diffusion procedure was optimized to provide a uniform distribution of iron over a crystal thickness (∼1 mm).

---

* Corresponding author. Tel./fax: +1 205 934 5318.
E-mail address: vfedorov@uab.edu (V.V. Fedorov).

0022-2313/$ - see front matter © 2011 Elsevier B.V. All rights reserved.
doi:10.1016/j.jlumin.2011.10.004

A controlled thermal diffusion of iron ions was used to fabricate co-doped Co:Fe:ZnSe and Co:Fe:ZnS samples with Fe concentration range of 8.5–19 × 10^{18} cm^{-3} and 0.5–10 × 10^{18} cm^{-3}, respectively, while cobalt concentration was maintained at 6.4 × 10^{18} cm^{-3} level for both crystals. Unpolarized emission spectra were measured at low temperatures with a close-cycle refrigerator system and a computer-controlled Acton Research "SpectraPro-750" spectrometer. Room temperature absorption measurements in visible and mid-IR spectral regions were performed with Shimadzu UV-3101PC and FTIR spectrophotometers. Kinetics and luminescence spectra of Fe:Co:ZnSe/S samples were measured under excitation with the radiation of Nd:YAG laser Raman shifted to 1.56 μm. The Raman Shifting was realized in D_2 Raman cell pumped by the 1.064 μm radiation of a single frequency Q-switched Nd:YAG laser with a repetition rate of 10 Hz and pulse duration of 7 ns. Direct optical excitation of Fe:ZnSe/S samples was performed using an actively Q-switched flashlamp pumped Er:Cr:YSGG laser operating at 2.8 μm. Signal acquisition, recording and treatment was provided by Tektronix TDS-380 (350 MHz bandwidth) digital averaging oscilloscope and Boxcar- Integrator SR250 (Stanford Research System).

3. Experimental results and discussion

A controlled thermal diffusion of iron ions was used to fabricate co-doped Co:Fe:ZnSe and Co:Fe:ZnS samples. The absorption spectra of experimental samples in the near and mid IR spectral range are depicted in Fig. 2. The maximum absorption coefficients of Co:ZnS and Co:ZnSe crystals at $^4A_2(F)\rightarrow{}^4T_1(F)$ transition were 6 and 5 cm^{-1}, respectively. The absorption coefficients of Co^{2+} ions in the near IR spectral range at $^4A_2(F)\rightarrow{}^4T_1(P)$ transition were ~8 times bigger for both crystals. The $^4A_2(F)\rightarrow{}^4T_2(F)$ transition of cobalt is symmetry forbidden and, hence, is barely visible in the absorption spectra of experimental samples. In addition to cobalt absorption bands in Co:Fe:ZnSe and Co:Fe:ZnS crystals, one can see an iron absorption band centered at ~3 μm and corresponding to the $^5E_2(D)\rightarrow{}^5T_2(D)$ iron transition. The maximum iron concentrations were equal to 19 × 10^{18} cm^{-3} and 10 × 10^{18} cm^{-3} for Co:Fe:ZnSe and Co:Fe:ZnS crystals, respectively. We observed ~20% decrease of Co^{2+} absorption bands intensity only in highly iron co-doped $C_{Fe} > 10^{19}$ cm^{-3}) crystals. It can be explained by multi-ion center-formation with different valence states of ions.

Room temperature luminescence of Co:ZnSe crystal under 1.56 μm excitation is shown in Fig. 3A. A broad luminescence band between 2.5 and 4 μm results from $^4T_2(F)\rightarrow{}^4A_2(F)$ radiative transition. The photoluminescence decay time of cobalt at this transition was reported to be ~200 μs [11] at RT. A room temperature luminescence spectrum at $^5T_2\rightarrow{}^5E$ transition of Fe^{2+} ions under direct excitation by 2.8 μm radiation is also shown in Fig. 3A. A dip at 4300 nm in photoluminescence spectra is caused by absorption of atmospheric CO_2. Due to temperature quenching at RT, the photoluminescence decay time of Fe^{2+} ions is equal to 0.38 μs [12]. Fig. 3B demonstrates time resolved spectra of Co:Fe:ZnSe co-doped samples under pulsed excitation into Co^{2+} absorption band. The energy transfer from cobalt to iron ions is clearly seen

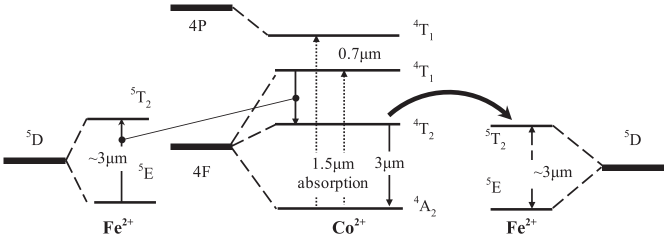

Fig. 1. Energy diagram of Co^{2+} and Fe^{2+} ions and possible energy transfer channels in ZnS/ZnSe crystals.

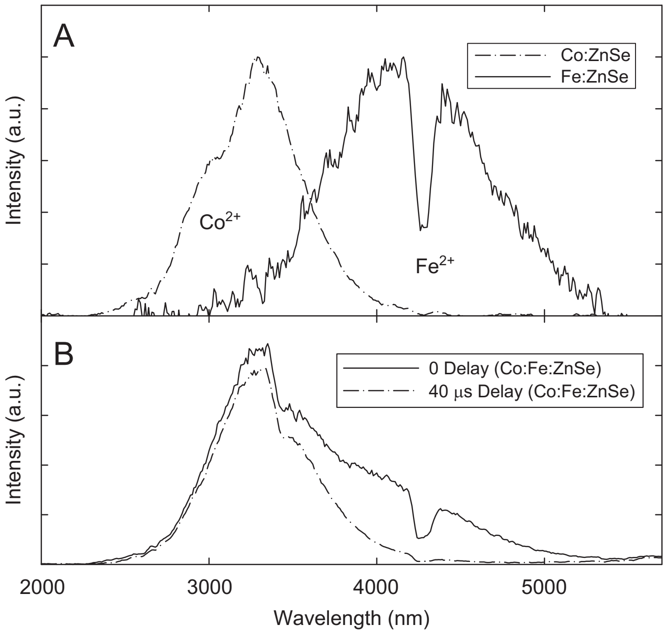

Fig. 3. (A) Room temperature luminescence spectra of Co:ZnSe (dash-dot line) and Fe:ZnSe (solid line) under direct excitation; (B) RT time resolved spectra of Co:Fe:ZnSe crystal under excitation at 1.56 μm measured with zero (solid line) and 40 μs (dash-dot line) time delays.

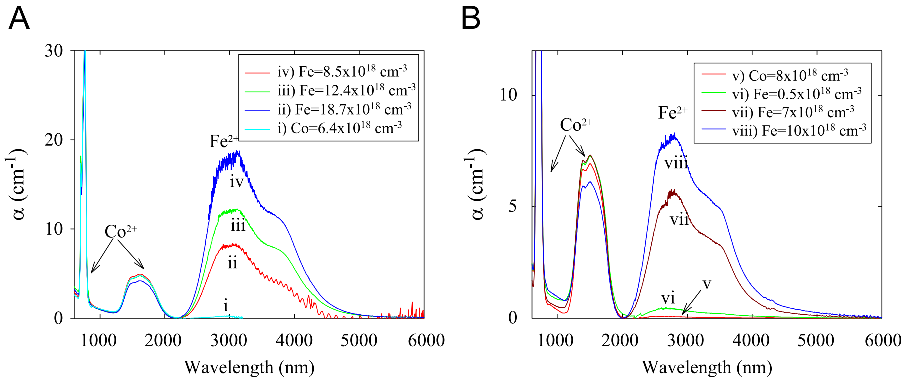

Fig. 2. Absorption spectra of co-doped Fe:Co:ZnSe (A) and; Fe:Co:ZnS (B) samples; (A) Co^{2+} concentration was fixed at 6.4 × 10^{18} cm^{-3} for all samples; Fe concentration varies over 8.5–19 × 10^{18} cm^{-3} ; (B) Co^{2+} concentration was fixed at 8 × 10^{18} cm^{-3}; Fe concentration varies over 0.5–10 × 10^{18} cm^{-3}.

from the PL spectrum measured with a zero delay with respect to the pump pulses. This spectrum consists of superposition of Co^{2+} and Fe^{2+} photoluminescence bands. However, the PL spectrum measured with 40 μs delay consists of only cobalt band.

Fig. 4 shows photoluminescence kinetics of PL signal of Co (6×10^{18} cm^{-3}):Fe(12×10^{18} cm^{-3}):ZnSe crystal under 1.56 μm excitation. RT kinetics measured at 3050 nm and 4050 nm demonstrated relaxation decays of Co^{2+} and Fe^{2+} ions, respectively. Both curves reveal a non-exponential decay at the initial stage. This behavior could be explained according to Forster–Dexter theory by the dependence of energy transfer rate in Co–Fe pairs on ions separation. As one can see from Fig. 4, the photoluminescence of Fe^{2+} ions decreases 1/*e* times over 0.5 μs interval, which is significantly shorter than Co^{2+} luminescence lifetime. It means that Co–Fe energy transfer rate in the closely packed Fe–Co pairs is very close to the RT lifetime of Fe^{2+} ions (0.38 μs); and, therefore, this mechanism should be sufficient for formation of the Fe^{2+} ions population inversion in these pairs. Within limits of temporal resolution of our registration system (100 ns), we have not observed Co^{2+} photoluminescence rise time at $^4T_2(F)\rightarrow{}^4A_2(F)$ transition at RT. Therefore, several microsecond kinetic of the Fe^{2+} luminescence could be due to energy transfer only from the $^4T_2(F)$ cobalt state. A non-exponential decay of cobalt ions can be due to a fast decay (<1 μs) in Co–Fe pair aggregates, while a long ($\sim$100 μs) tale of Co kinetics can be due to Co–Fe energy migration from non-paired cobalt ions.

Fig. 5 demonstrates kinetics of photoluminescence of Co:Fe:ZnS co-doped crystal measured at 3050 nm and 4500 nm. For these experiments, Co:Fe:ZnS crystal with cobalt and iron concentrations of $C_{Co}=6\times10^{18}$ cm^{-3} and $C_{Fe}=12\times10^{18}$ cm^{-3} was excited at $^4A_2(F)\rightarrow{}^4T_2(F)$ cobalt transition by 1.56 μm radiation. The PL kinetics at 4500 nm were non-exponential for room and low temperatures. The decay of PL signal at room temperature was shorter than in ZnSe crystal. The photoluminescence signal of Fe^{2+} ions decreases by a factor of 10 during 1 and 2 μs in ZnS and ZnSe crystals, correspondingly.

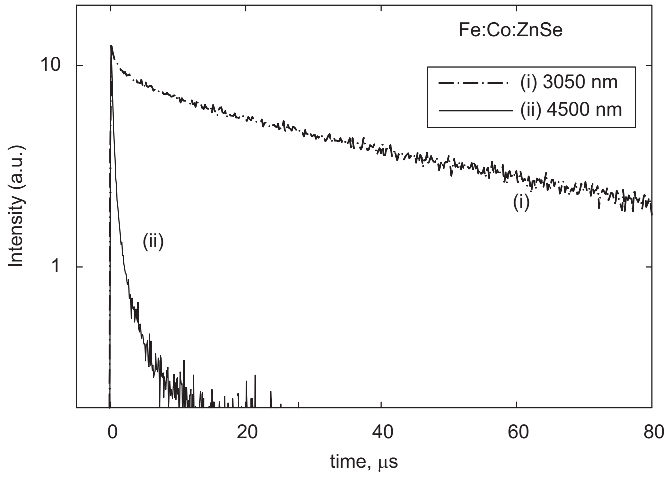

Fig. 4. RT photoluminescence kinetics of Co (6×10^{18} cm^{-3}):Fe(12×10^{18} cm^{-3}): ZnSe crystal measured under excitation at 1.56 μm at (i) 3050 nm and (ii) 4500 nm.

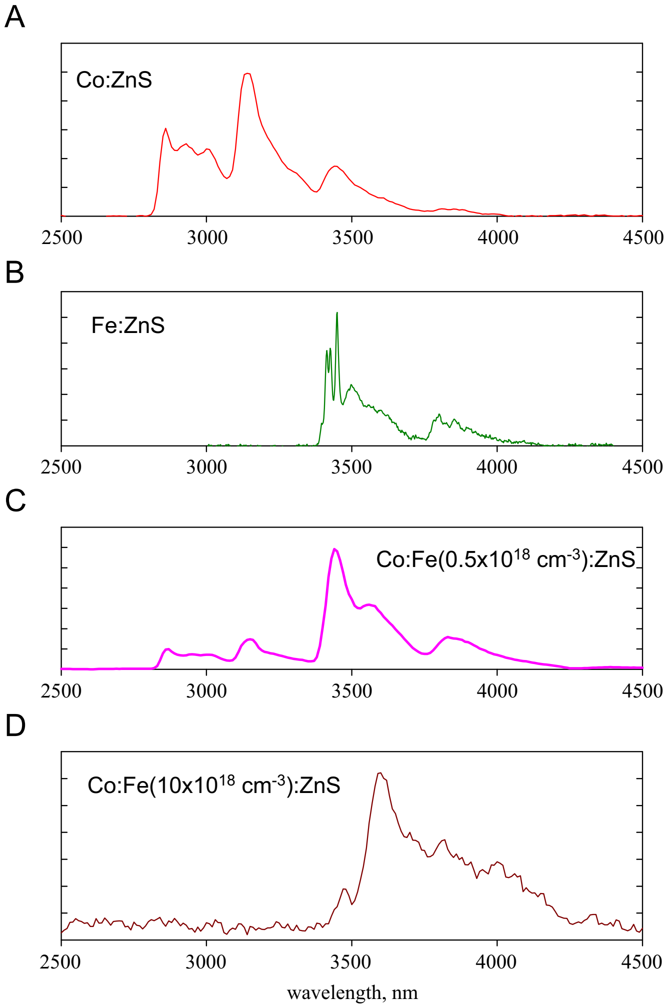

Fig. 6. Mid-IR luminescence spectra of iron and cobalt co-doped ZnS crystals at $T=14$ K.

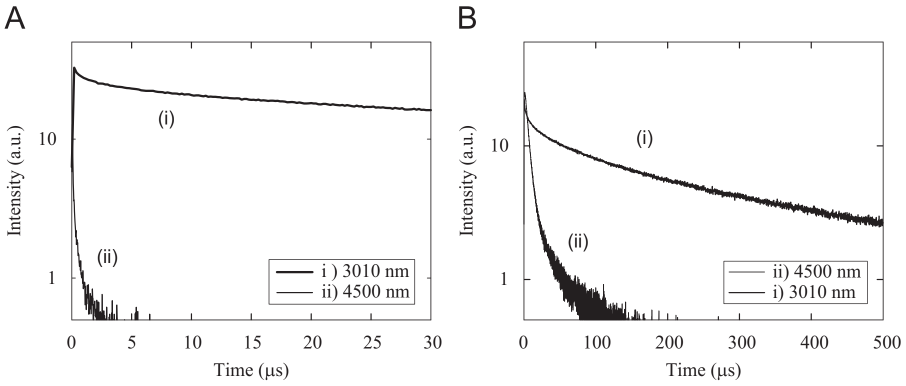

Fig. 5. Photoluminescence kinetics of Co (6×10^{18} cm^{-3}):Fe (7×10^{18} cm^{-3}):ZnS crystal measured under excitation at 1.56 μm at 3050 nm (i) and 4500 nm (ii); at $T=300$ K (A) and $T=14$ K (B).

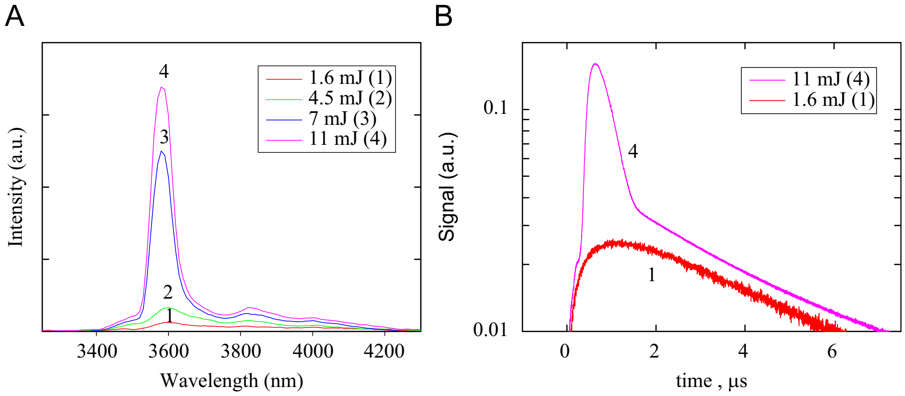

Fig. 7. (A) Mid-IR luminescence spectra of Co:Fe:ZnS crystal at different pump energies at $T=14$ K, (B) Co:Fe:ZnS crystal PL kinetics for different pump energies below (i) and above (ii) laser threshold.

Fig. 6 shows luminescence spectra of several Co and Fe co-doped ZnS crystals measured at 14 K. The first plot (A) demonstrates typical Co^{2+} luminescence under 1.56 µm excitation with characteristic luminescence peaks at around 2800 and 3100 nm. The third plot (C) shows luminescence spectra of Co:Fe:ZnS crystal with a low iron concentration 0.5×10^{18} cm^{-3} under the same 1.56 µm excitation. As one can see from this graph, in addition to Co^{2+} luminescence, there is a strong Fe^{2+} luminescence with characteristic peaks at 3440 nm, 3570 nm, and 3820 nm. For comparison, the luminescence of the Fe:ZnS sample under direct excitation of the iron ions at 2.9 µm measured at 14 K is depicted in the second plot (B). The fourth plot (D) shows luminescence spectra of Co:Fe:ZnS crystal under 1.56 µm excitation with 50 times bigger iron concentration. As one can see, there is no Co^{2+} luminescence in this crystal. The measured luminescence spectrum shows only Fe^{2+} bands slightly red-shifted in comparison with the low doped sample spectrum. This result proves that there is a fast energy transfer from Co^{2+} to Fe^{2+} ions in this crystal and we used this crystal for the following laser experiments.

A high gain in a highly doped Co:Fe:ZnS crystal enabled experiments on lasing under 1.56 µm pumping even without an external cavity. For these experiments we used Co:Fe:ZnS crystal ($10\times10\times1.2$ mm^3) with 0.5×10^{18} cm^{-3} and 10×10^{18} cm^{-3} concentrations of cobalt and iron, respectively. The pump radiation was slightly focused in the spot with $d\sim3$ mm diameter. The crystal was placed in a close-cycle refrigerator system operating over 14 K–300 K temperature range.

Two basic experiments on pump energy dependence of luminescence kinetics and luminescence spectra were performed to demonstrate Fe^{2+} lasing via effective energy transfer from Co^{2+} ion. A positive feedback for Fe oscillation was realized due to Fresnel reflections from the crystal facets providing 18% feedback reflectivity from each surface. The large resonator Fresnel Number $N_F=d^2/L\lambda\sim10^4$ provides minimum diffraction losses in the cavity.

The results of lasing experiments are depicted in Fig. 7. Fig. 7A demonstrates PL spectra of Co:Fe:ZnSe crystal for different pump energies. As one can see in Fig. 7A, at low pump energy the measured PL spectra were typical for luminescence of iron ions. The dependence of PL spectrum profile on the pump energy demonstrated a threshold behavior, as shown in Fig. 7A, accompanied by appearance of stimulated emission band around 3850 nm. The laser threshold was measured to be 6 mJ. The change of luminescence profile above laser threshold was accompanied by a shortening of PL kinetics as shown in Fig. 7B. For a low pump energy one can see a low temperature Fe^{2+} kinetics with luminescence rise time $\tau\sim1$ µs followed by exponential decay with ~2.5 µs lifetime. Above laser threshold, the kinetics demonstrate a typical laser spike with ~200 ns pulse duration followed by below threshold luminescence kinetics. The threshold dependence of emission, a significant line narrowing, and a lifetime shortening are clear evidence of Co:Fe:ZnSe lasing via Co→Fe energy transfer mechanism. The laser threshold reveals a strong dependence on temperature. The highest temperature, where we were able to demonstrate laser oscillation with a positive feedback due to Fresnel reflections was 21 K.

4. Conclusions

The energy transfer to Fe^{2+} ($^5T_2$) ions under 1.56 µm Co^{2+} excitation at $^4A_1\rightarrow{}^4T_1$ transition was investigated. The new excitation mechanism for Fe^{2+} lasers via energy transfer from Co^{2+} to Fe^{2+} was demonstrated in the cavity with a positive feedback provided by Fresnel reflections from the crystal facets. Demonstrated Co–Fe energy transfer processes open a new pathway for pumping mid-IR Fe based lasers with the use of commercially available near infrared pump lasers. Laser oscillation at 3.6 µm over 14–21 K temperature range was demonstrated using Co:Fe:ZnS crystal. Further, optimization of co-dopant concentrations is required to achieve laser threshold at room temperature.

Acknowledgements

The authors would like to acknowledge funding support from National Science Foundation EPS-0814103, ECCS-0901376, and Kirtland AFB/UAB contract FA9451-10-C-0254/P00002.

The work reported here partially involves intellectual property developed at the University of Alabama at Birmingham. This intellectual property has been licensed to the IPG Photonics Corporation. The UAB co-authors declare competing financial interests.

References

[1] S. Mirov, V. Fedorov, I. Moskalev, D. Martyshkin, C. Kim, Laser Photon. Rev. 4 (2010) 21.
[2] V.V. Fedorov, S.B. Mirov, A. Gallian, D.V. Badikov, M.P. Frolov, Yu.V. Korostelin, V.I. Kozlovsky, A.I. Landman, Yu.P. Podmar'kov, V.A. Akimov, A.A. Voronov, IEEE J. Quantum Electron. 42 (2006) 907.
[3] J.J. Adams, C. Bibeau, R.H. Page, D.M. Krol, L.H. Furu, S.A. Payne, Opt. Lett. 24 (1999) 1720.
[4] A.A. Voronov, V.I. Kozlovsky, Yu.V. Korostelin, A.I. Landman, Yu.P. Podmar'kov, Ya.K. Skasyrsky, M.P. Frolov, IEEE J. Quantum Electron. 38 (2008) 1113.

[5] J. Kernal, V.V. Fedorov, A. Gallian, S.B. Mirov, V.V. Badikov, Opt. Express. 13 (2005) 10608.
[6] M.E. Doroshenko, H. Jelínková, P. Koranda, J. Sulc, T.T. Basiev, V.V. Osiko, V.K. Komar, A.S. Gerasimenko, V.M. Puzikov, V.V. Badikov, D.V. Badikov, Laser Phys. Lett. 7 (2010) 38.
[7] NoSoung Myoung, Dmitri V. Martyshkin, Vladimir V. Fedorov, Sergey B. Mirov, Opt. Lett. 36 (2011) 94.
[8] N.C. Ming Luo, Utpal N. Giles, Yunlong Roy, Cui, Arnold Burger, J. Appl. Phys. 98 (2005) 083507.
[9] A. Karipidou, H. Nelkowski, G. Roussos, J. Cryst. Growth 59 (1932) 307.
[10] Crystal field engineering of solid state laser materials, Brian Henderson, Ralph H. Bartram (Eds.), Cambridge University Press, 2000, pp 196–200.
[11] L.D. DeLoach, R.H. Page, G.D. Wilke, S.A. Payne, W.F. Krupke, IEEE J. Quantum Electron. 32 (1996) 885.
[12] NoSoung Myoung, Dmitri V. Martyshkin, Vladimir V. Fedorov, Alan Martinez, Sergey B. Mirov, Proc. SPIE 7912 (2011) 79121C.